

## FLUXGATE SENSORS BASED ON MAGNETIC MICROWIRES FOR WEAK MAGNETIC FIELDS MEASUREMENT

Jozef Hudák\* – Pavol Lipovský\* – Ján Bajús\* – Andrej Čverha\*  
– Peter Klein\*\* – Rastislav Varga\*\* – Jozef Onufer\*\*\* – Ján Ziman\*\*\*

The dominating trend in the reduction of dimensions, power consumption and cost of sensors in conjunction with the requirement of their precision and dynamics improvement and also in the range of the measured fields leads in the area of the fluxgate magnetometers to the replacement of the conventional sensors by their microwire substitutions. The article summarizes results of the transfer characteristics measurements of the developed microwire fluxgate sensors. These sensors are designed for the vector measurements of the low frequency weak magnetic fields. The basis for a determination of the sensors' characteristics lies in the repeated measurements during the one second time intervals in the defined operating points and also in the measurement of the differentials of the time intervals obtained during the alternating magnetizations in the defined magnetic field. Based on the measured static and dynamic transfer characteristics microwire fluxgate sensors with a different chemical composition and core geometry from various manufacturers are compared. The results of the experiments creates the basis for a consideration of the possibility to replace currently used amorphous ribbon core sensors in the VEMA series magnetometers with the fluxgate sensors based on magnetic microwires.

Keywords: microwire, sensor, magnetometer, transfer characteristics

### 1 INTRODUCTION

Digital magnetometers of VEMA (Vector Magnetic Analyzer) series, developed and realized by the researchers at the Department of Aviation Technical Studies at the Faculty of Aeronautics have over 20 year history. Currently the relax-type vector magnetometers for measurement of weak magnetic field vector components in the range of  $\pm 100 \mu\text{T}$  with resolution 1–2 nT/count (LSB) and the sampling frequency of 500 Hz or 1000 Hz have been developed [1-3], which are used not only in industrial, but also in laboratory applications.

The principle of a magnetic field measurement by VEMA series magnetometers is in alternating saturation of the core and consequent measurement of relaxation time intervals, when the probe relaxes into the value of external, measured magnetic field. This measurement of the magnetic field is thus based on the measurement of transition effects length in the core of the probe, what results in the pulse-width modulated digital signal.

The VEMA sensor has the form of two concentric coils, sensor length is 100 mm and with a diameter of 10 mm. The core is made from amorphous ribbons from VITROVAC 6030 material. This sensor has relatively large geometrical dimensions, but its dimensions allow a good evaluation of relaxation transition effects and a precise measurement of a magnetic field vector projection into the axis of the sensor.

Currently, in compliance with the trends of reduction of the dimensions, decreasing of power consumption and increasing the performance of sensoric systems, in the

area of the weak magnetic field measurement magnetic microwire sensors seem to have perspective future [4-7].

The aim of our work is in evaluation of their basic properties in comparison with the relax-type sensors that have been currently used in the practice. Both of these sensors are pulse-type fluxgate sensors.

### 2 MEASUREMENT OF TESTED SENSORS CHARACTERISTICS

For testing purposes we chose self-bearing sensor consisting of concentric coupled coils with 20 mm length (Fig. 1). Three types of materials from different manufacturers with 10 mm and 20 mm lengths were tested.

The first one (marked as S1) was a microwire sample from INSTITUTE ELIRI, with a chemical composition  $\text{Co}_{65.48}\text{Fe}_{4.12}\text{Si}_{11}\text{B}_{16}\text{Cr}_{3.4}$ . It was the unannealed glass coated microwire with the outer diameter of 28  $\mu\text{m}$  and the core diameter of 19  $\mu\text{m}$ . The second type (S2) was a microwire sample from UNITIKA, type 30DC2T, with the 30  $\mu\text{m}$  diameter, unannealed and without glass coating. The third microwire sample type (S3) with composition  $\text{Co}_{69.4}\text{Fe}_{3.7}\text{Si}_{11}\text{B}_{15.9}$  was obtained from the Pavol Jozef Šafárik University in Košice. It was glass coated, with outer/core diameters 24  $\mu\text{m}$  / 14  $\mu\text{m}$ , and it was annealed in 300°C for 60 minutes to achieve required hysteresis loop shape with steep transition in the middle. The hysteresis loops for tested microwires are shown in Fig. 2. These loops were measured in specialized laboratory at the Department of Physics, Faculty of Electrical Engineering and Informatics, Technical University of Košice by the static induction method described in [8].

\* Technical University of Košice, Faculty of Aeronautics, Department of Aviation Technical Studies, Rampová 7, 041 21 Košice, Slovakia, jozef.hudak@tuke.sk, pavol.lipovsky@tuke.sk, jan.bajus@tuke.sk, cverha.a@gmail.com

\*\* Pavol Jozef Šafárik University in Košice, Institute of Physics of the Faculty of Science, Department of Condensed Matter Physics, Park Angelinum 9, 041 54 Košice, Slovakia, peter.klein@upjs.sk, rastislav.varga@upjs.sk

\*\*\* Technical University of Košice, Faculty of Electrical Engineering and Informatics, Department of Physics, Park Komenského 2, 042 00 Košice, Slovakia, jozef.onufer@tuke.sk, jan.ziman@tuke.sk

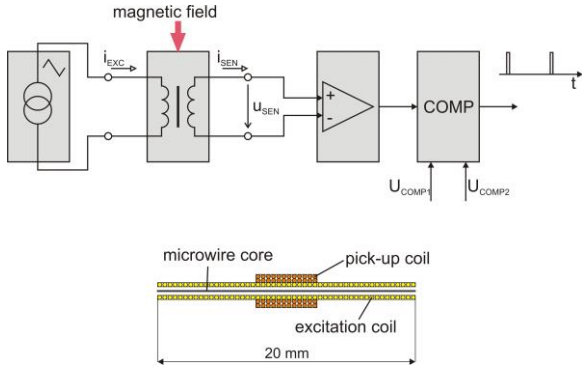


Fig. 1. Block diagram of microwire sensor principle and tested sensor geometries

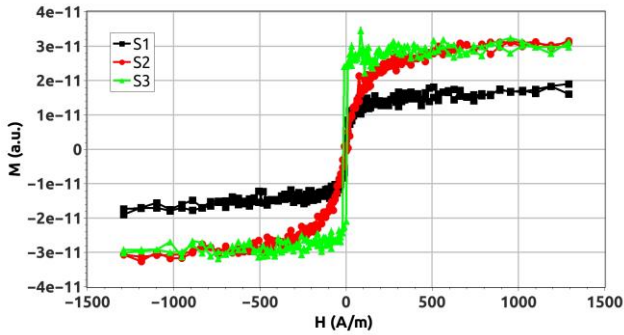


Fig. 2. Hysteresis loops shapes

Properties comparisons of the listed microwire sensors were based on evaluation of time intervals of induced peaks occurrences that are proportional to alternating magnetization of sensor core [9], which is influenced by external magnetic field as shown in Fig. 3, where  $H_{exc}$  is the amplitude of the excitation field,  $H_x$  is the measured field,  $H_c$  is the coercivity of the microwire core,  $T$  is the half period of the excitation signal,  $t^+$  and  $t^-$  are the measured time intervals.

$$t^+ = \frac{T}{2H_{exc}}(H_c + H_{exc} - H_x) \quad (1)$$

$$t^- = \frac{T}{2H_{exc}}(H_c + H_{exc} + H_x) \quad (1)$$

The output of the sensor is in the form of pulse-position modulation, time intervals and  $t^+$  and  $t^-$  (1) are measured [9]. The external measured field  $H_x$  can be expressed from (1)

$$H_x = -\frac{H_{exc}}{T}(t^+ - t^-) \quad (2)$$

In our case variant measurement chain as it is shown in Fig. 4 was used. The excitation part consisted from function generator and  $U/I$  converter connected to the excitation coil of the microwire sensor. The excitation current signal had amplitude of 10 mA.

Voltage projection of the triangle wave excitation current was fed into the pair of comparators to generate start pulses for counters with 200 MHz clock frequency. The pick-up coil was connected through the instrumentation amplifier AD620 to the second pair of comparators used for generation of stop pulses for counters.

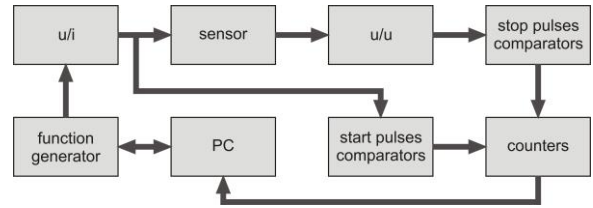


Fig. 4. Block diagram of the measurement chain

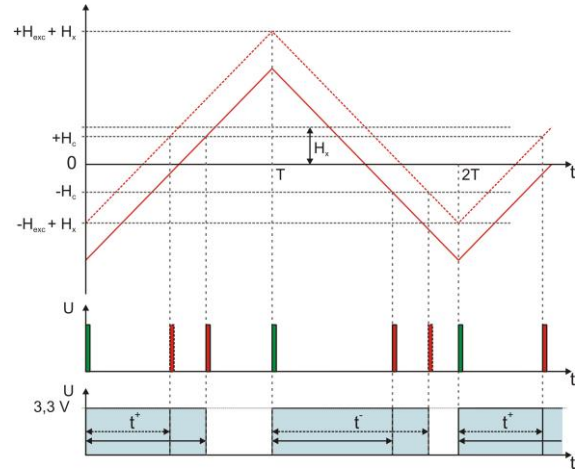


Fig. 3. Microwire sensor principle

Determination of the fundamental system and statistical parameters of the tested sensors, that are included in static and dynamic transfer characteristics, is expressed by general mathematical model of static transfer characteristics:

$$\Delta t = Kb + a + N() + K_{ME}b\Delta T_{AE} + K_{MS}b\Delta T_{AS} + K_{IE}\Delta T_{AE} + K_{IS}\Delta T_{AS} \quad (3)$$

The output signal from sensor  $\Delta t$  is not only a function of the measured quantity (time-varying magnetic flux density  $b$ ), but it also depends on driving parameters (shape, amplitude and frequency of the excitation current  $i_{exc}$ ) [10] and interfering and modifying quantities (temperature of electronics  $T_{AE}$  and temperature of sensor  $T_{AS}$ ). This influence is in (3) included in coefficients (sensitivity  $K$ , offset  $a$ , modifying influences of ambient temperature on electronics  $K_{ME}$  and sensor  $K_{MS}$ , interfering influence of environment on electronics  $K_{IE}$  and sensor  $K_{IS}$ ) and also in functions (non-linearity  $N$ , transfer  $G$ ).

The measurement of tested sensors transfer characteristics was realized in environmental conditions of a general laboratory. The ambient temperature was stabilized at 20 °C and was the same for electronics and sensor ( $T_{AE} = T_{AS} = T_A$ ). The reference temperature for sensor was specified to 20 °C, so  $\Delta T_{AE} = \Delta T_{AS} = \Delta T_A = 0$  and (3) simplifies (in initial approach) to

$$\Delta t = Kb + a + N() \quad (4)$$

Measured magnetic field, generated by Helmholtz coils, was interfered by 50 Hz magnetic field from power grid and measurement devices. The observation interval  $t_0$

during the measurements in one point of transfer characteristics was 1 s, what corresponds to taking 500  $t+$  and  $t-$  time intervals by excitation frequency of 500 Hz.

### 3 EXPERIMENTAL RESULTS

The dependency of the induced voltage peak shape on the magnitude of the measured magnetic field (specifying the operation point on BH characteristics of the sensor core) allows definition of the measurement range. From the measured values and considering the shapes of induced peaks in the sensing winding, it is possible to effectively utilize the measurement range  $\pm 250 \mu\text{T}$  with the specified measurement chain with a negligible non-linearity (non-linearity and hysteresis are smaller than standard deviation of measured value  $\sigma$ ). Further extension of the measurement range to  $\pm 500 \mu\text{T}$  brings increase of non-linearity error that has to be compensated.

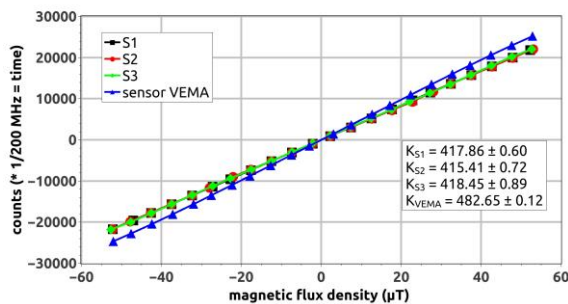


Fig. 5. Transfer characteristics of S1, S2, S3 and VEMA sensors

The transfer characteristics of S1, S2, S3 sensors with the excitation current amplitude of 10 mA and the VEMA magnetometer measured  $\pm 50 \mu\text{T}$  range with the measurement chain from Fig. 4 with subtracted offsets  $a$  are shown in Fig. 5. The  $a$  parameter has for VEMA sensor values around 500 counts, mainly depending on the components in the relaxation circuits, while considering the microwire sensor principle, the offset mainly depends on the generator signal offset and during the measurements were observed very low values below 10 counts.

Table 1. Sensitivities of the tested sensors

Sensor	Sensitivity (counts/ $\mu\text{T}$ )
VEMA	$482.65 \pm 0.12$
S1	$417.86 \pm 0.60$
S2	$415.41 \pm 0.72$
S3	$418.45 \pm 0.89$

These characteristics are for microwire sensors well approximated by linear functions (the non-linearity is smaller than the variance of measured values). The VEMA sensor had full scale non-linearity of 0.5 %. Sensitivities of tested sensors in counts/ $\mu\text{T}$  are listed in Table 1. They are comparable to the sensitivity of VEMA magnetometer. The ranges of outputs corresponding to the input

range  $\pm 50 \mu\text{T}$  are for S1, S2 and S3 sensors approximately  $\pm 21\,000$  counts and for VEMA magnetometer  $\pm 24\,000$  counts.

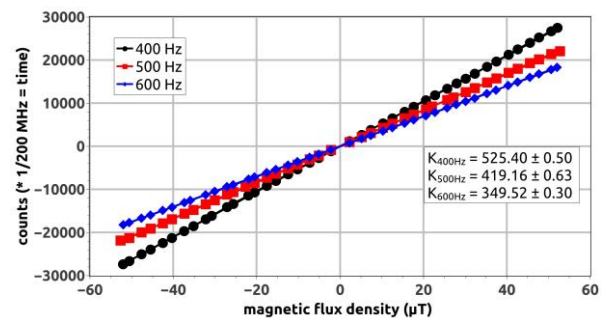


Fig. 6. Dependency of S3 sensor sensitivity on excitation field frequency

The example static transfer characteristics for S3 sensor shown in Fig. 6 were measured with the same excitation current amplitude, but with different frequencies: 400 Hz, 500 Hz and 600 Hz. In this excitation frequency range the sensitivity was not influenced by the properties of the tested microwires; its change is indirectly proportional to the excitation frequency change and corresponds to the theoretical assumptions, the highest sensitivity was at  $f_{EXC} = 400$  Hz. Identical behaviour was observed with sensors S1 and S2.

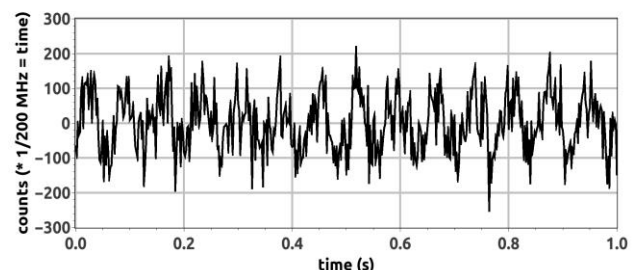


Fig. 7. Time development of sensed signal from S3 sensor with 200 nT stimulation signal

To consider the resolution of the tested sensors measurements of sensors output signal with stimulation sine wave signal with 200 nT amplitude and 14 Hz frequency were realized. In the time development from Fig. 7 and frequency spectrum from Fig. 8 is this stimulation signal clearly visible also with the interfering 50 Hz industrial frequency in the frequency range of the sensor.

After turning off the stimulation signal and 50 Hz interference filtering, the basic analysis of measurement chain noise with S3 sensor gives following results: mean value of signal time development during  $t_0 = 1$  s is zero, probability density is well approximated by Gaussian distribution. So the noise of the measurement chain with the S3 sensor can be considered as random white noise. Almost identical results were obtained with S1 and S2 sensors. The potential sources of the noise could be the electronics [11], but also the noise of the microwire itself is not negligible [9].

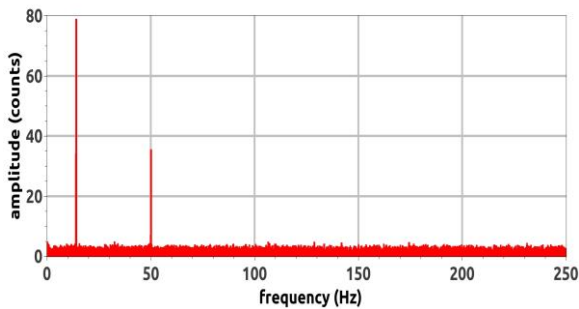


Fig. 8. Frequency spectrum of sensed signal from S3 sensor with 200 nT / 14 Hz stimulation signal

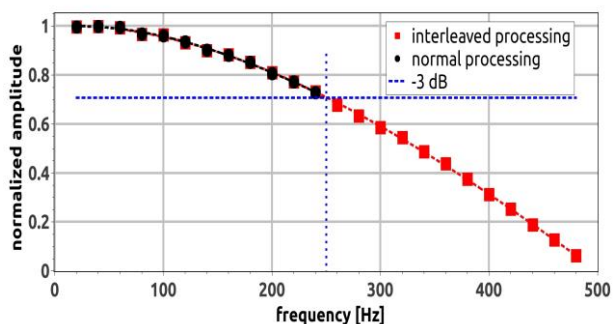


Fig. 9. Frequency characteristics of S3 sensor

The frequency characteristics of the tested sensors are identical (in Fig.9 is shown frequency characteristics for the measurement chain with S3 sensor) and correspond to the theoretical assumptions. The frequency range from DC to 250 Hz is identical with VEMA series magnetometers operating with the 500 Hz sampling frequency. The measurement of time intervals  $t_+$  and  $t_-$  for positive and negative magnetization allows evaluation of the measurement with the doubled frequency, the frequency range remains unchanged, but higher frequencies are more suppressed.

#### 4 CONCLUSIONS

Measurements realized with S1, S2, S3 sensors tested in the same measurement chain proved the possibility to achieve similar sensitivities as the VEMA sensors with microwire sensors in the same measurement range as it is shown in Table 1. Because of the physical principle, the microwire sensors can achieve better offset and non-linearity parameters. The frequency range for the tested sensors is the same for both, the VEMA and the microwire sensors, DC to 250 Hz.

Microwire sensors also bring other advantages concerning lower power consumption, decrease of geometrical dimensions and widening the application possibilities. But the relax-type magnetometers still have advantage in less complicated electronics and their sensors can be placed on long connection wiring, in industrial practice up to 50 m that connects the transducer with the main electronics.

#### Acknowledgement

This work has been supported by the grant agencies of Slovak Republic grants KEGA 028TUKE-4/2013, VEGA 1/0286/13 and APVV-0266-10.

We would like to thank Pavol Jozef Šafárik University in Košice from Slovakia, UNITIKA Ltd. from Japan and Institute ELIRI from Moldavia for provision of the microwires samples.

#### REFERENCES

- [1] PRASLICKA, D.: A Relax-Type Magnetometer Using Amorphous Ribbon Core, IEEE Transactions on Magnetics, 30/2, p. 934-935, 1994. ISSN 0018-9464.
- [2] HUDÁK, J. — BLAŽEK, J. — PRASLIČKA, D. — MIKITA, I. — LIPOVSKÝ, P. — GONDA, P.: Sensitivity of VEMA-04.1 magnetometer, Journal of Electrical Engineering, Vol. 61, Issue 7/s, p. 28 – 31, 2010. ISSN 1335-3632.
- [3] MARCIN, J. — KLINDA, A. — SVEC, P. — PRASLICKA, D. — BLAŽEK, J. — KOVAC, J. — SVEC, P. — Sr., SKORVANEK, I.: Melt-Spun Fe-Co-B-Cu Alloys With High Magnetic Flux Density for Relax-Type Magnetometers. In IEEE Transactions on Magnetics, Vol. 46, Issue 2, 2010, p. 416-419. ISSN 0018-9464.
- [4] KLEIN, P. — VARGA, R. — VOJTANIK, P. — KOVAC, J. — ZIMAN J. — BADINI-CONFALONIERI, G. A. — VAZQUEZ, M.: Bistable FeCoMoB microwires with nanocrystalline microstructure and increased Curie temperature, Journal of Physics D-applied Physics, Vol. 43, Issue 4, 2010. ISSN 0022-3727.
- [5] IOAN, C. — CHIRIAC, H. — DIACONU, E.D. — MOLDOVANU, A. — MOLDOVANU, E. — MACOVEI, C.: High-resolution fluxgate sensing elements using Co<sub>68</sub>,25Fe<sub>4</sub>,5Si<sub>12</sub>,25B<sub>15</sub> amorphous material, Journal of Optoelectronics and Advanced Materials, Vol. 4, Issue 2, 2002, p. 319 – 324. ISSN 1454-4164.
- [6] HUDÁK, R. — VARGA, R. — HUDÁK, J. — PRASLIČKA, D. — BLAŽEK, J. — POLÁČEK, I. — KLEIN, P.: Effect of the fixation patterns on magnetic characteristics of amorphous glass-coated sensoric microwires. In Acta Physica Polonica A, Proceedings of the 15th Czech and Slovak conference on Magnetism, Vol. 126, no. 1, 2014, p. 417-418. ISSN 0587-4246.
- [7] DRAGANOVÁ, K. — BLAŽEK, J. — PRASLIČKA, D. — KMEC, F.: Possible Applications of Magnetic Microwires in Aviation. In Fatigue of Aircraft Structures, Warsaw, Institute of Aviation Scientific Publications, 2013, p. 12-17. ISSN 2081-7738.
- [8] ZIMAN, J. — ZAGYI, B.: DC-magneto-resistance in surface crystallized FeSiB amorphous wire, Journal of Magnetism and Magnetic Materials, Vol. 169, 1997, p. 98-104. ISSN 0304-8853.
- [9] PRASLIČKA, D. — ŠMELKO, M. — BLAŽEK, J. — HUDÁK, J. — LIPOVSKÝ, P. — FLACHBART, N.: Advanced method for magnetic microwires noise specification, Acta Physica Polonica A, CSMAG'13 : 15th Czech and Slovak Conference on Magnetism, Book of Abstracts and Programme : S. 94, June 17. - 21., 2013, Košice, UPJŠ, 2013, Vol. 126, no. 1 (2014), p. 86-87. ISBN 978-80-8152-015-0 - ISSN 1898-794X.
- [10] ANDÓ, B. — BAGLIO, S. — BULSARA, A. — SACCO, V.: Effects of driving mode on RTD-FluxGate performances. In Conference Record - IEEE Instrumentation and Measurement Technology Conference, Vol. 2, 2004, 1419-1423. ISSN 1091-5281.
- [11] KOREPANOV, V. — MARUSENKOV, A.: Modern flux-gate magnetometers design, International Conference on Magnetism, Geomagnetism and Biomagnetism : Conference Proceedings, Sezana, 2008. p. 31-36.

Received 30 November 2015